RESEARCH

Studies on dielectric and magnetic properties of $CaCu_3Ti_3MnO_{12}$ ceramic synthesized via semi-wet route

Santosh Pandey[1] · Atendra Kumar[1] · N. B. Singh[2] · K. D. Mandal[1]

Abstract

$CaCu_3Ti_3MnO_{12}$ (CCTMO) ceramic has been successfully synthesized by the semi-wet route and sintered at 1223 K for 8 h, which is confirmed by XRD analysis to ensure $CaCu_3Ti_3MnO_{12}$ (CCTMO) phase formation. The microstructure, phase-structure, and thermal behavior were examined by scanning electron microscopy (SEM), X-ray diffraction (XRD), and thermogravimetric analysis (TGA), respectively. After Mn-doping, the dielectric constant decreases from 10^4 to 10^2. The particle size as well as grain size measured by TEM and SEM techniques which were found to be 43.76 ± 10 nm and 1.46 μm, respectively. The route mean square and average roughness observed by atomic force microscope (AFM) analysis were 0.141 μm and 0.109 μm, respectively. The temperature-dependent ferromagnetic nature of CCTMO ceramic was confirmed by zero field cooled (ZFC), field cooled (FC), and M-H hysteresis curves. The investigated magnetic property of CCTMO confirmed paramagnetic behavior at 300 K and ferromagnetic behavior at 5 K. The dielectric constant (ε^r) increases when temperature increases, although dielectric constant and dielectric loss were observed 100 and 0.1, respectively.

Keywords Semi-wet route · Dielectric properties · Magnetic properties

Introduction

$ACu_3Ti_4O_{12}$ (where A = $Y_{2/3}$, $Bi_{2/3}$, $Gd_{2/3}$) type of perovskite oxide was discovered in 1967 and their accurate structure was determined in 1979 [1] which was found to have the ability to produce high dielectric constant. Over the last decade, Scientists have been using $BaTiO_3$, $Pb(Mg_{1/3}Nb_{2/3})O_3$(PMN), and $Pb(Zn_{1/3}Nb_{2/3})O_3$(PZN) as a relaxer ferroelectric which possess high permittivity constant ($\varepsilon r \approx 10^2 – 2 \times 10^4$) [2]. The main problems with BaTiO3 are ferroelectric nature; i.e., it shows a phase transition with increasing temperature, and the dielectric constant varies with increasing temperature making it a poor candidate as a capacitor material. Due to these drawbacks, Subramanian et al. discovered $CaCu_3Ti_4O_{12}$ (CCTO) complex perovskite oxide with a high dielectric constant which has been utilized for analogous studies [3, 4]. In previous studies, it has been reported that the microstructure and impedance properties of CCTO ceramic are greatly influenced by the synthesis route [5, 6]. The complex perovskite-type of CCTO material shows numerous applications including in ceramic capacitor, dynamic random-access memory, transducers, microelectronic, microwave devices, and in other electronic equipment due to its high thermally stability and giant permittivity ($10^4–10^5$) in the temperature range 100–600 K without any structural phase transition [7–9]. CCTO-based ceramic has a body-centered cubic structure with a lattice parameter of 7.391 A° and space group Im3 [10, 11]. Usually, a high dielectric constant value is displayed by ferroelectric substances and this is connected to atomic displacement with non-Centro symmetrical shape [3]. The permittivity and magnetic properties of CCTO ceramic were improved by the doping of different cationic substituents at Cu and Ti-site in $CaCu_3Ti_4O_{12}$ [12]. The giant dielectric constant of CCTO ceramic was widely explained by grain boundary barrier layer (GBBL) capacitor models on the grain boundaries between semiconducting grains [9]. CCTO ceramic studies by impedance spectroscopy reveal that it is heterogeneous in nature containing semiconducting grains and insulating grain boundaries [13, 14]. The activation energy of CCTO was found to be around 0.1 eV [13]. It is reported that

✉ K. D. Mandal
kdmandal.apc@itbhu.ac.in

1 Department of Chemistry, Indian Institute of Technology (BHU), Varanasi, UP 221005, India

2 Department of chemistry and biochemistry, University of Maryland Baltimore County, Baltimore, MD 21250, USA

high permittivity value of CCTO ceramic is not intrinsic but due to extrinsic characteristics related to their microstructure [15]. Some modifications have been applied for the upgrade of dielectric properties of CCTO ceramic. Since last few years currently, the well-known process is partial substitution on the Cu and Ti site which refine the permittivity and give assistance to understand the genesis of high permittivity response in CCTO ceramic [16, 17]. The dielectric response was also affected by the shape of grains and grain boundaries [18, 19]. Mn-doped CCTO significantly decreases the grain boundary resistance, permittivity, and dielectric loss of CCTO ceramic due to decrease in the grain size for increasing the density on grain boundaries [20, 21]. In this work, we have synthesized the CCTMO through semi-wet route and reported their magnetic, dielectric properties and their microstructures. This procedure has the advantage of improving permittivity, dielectric loss, and magnetic response of CCTMO ceramic.

Experimental

Material synthesis

CCTMO was synthesized through semi-wet route. In this method, chemicals calcium nitrate, $Ca(NO_3)_2 \cdot 4H_2O$ (98% Merck, India), copper nitrate, $Cu(NO_3)_2 \cdot 3H_2O$ (99% Merck, India), manganese acetate, $Mn(CH_3COO)_2 \cdot 4H_2O$ (99% Merck, India), and titanium oxide, TiO_2 (99% Merck, India) were taken in stoichiometric amount in molar ratio. The solution of $Ca(NO_3)_2 \cdot 4H_2O$, $Cu(NO_3)_2 \cdot 3H_2O$, and $Mn(CH_3COO)_2 \cdot 4H_2O$ were prepared in distilled water. All the solutions were mixed together in a beaker and stoichiometric amount of solid TiO_2 was added in solution. The calculated amount of citric acid (99.5%, Merck India) equivalent to metal ions was dissolved in distilled water and mixed with the solution. The resulting solution was heated on a hot plate magnetic stirrer at 343–353 K to evaporate water and allows for self-ignition. A fluffy mass of CCTMO powders was obtained after removal of a lot of gases. Citric acid used as a complexing agent that acts as fuel in the ignition step. The resulting CCTMO powder was ground with the help of agate and mortar to make a fine powder. The powder was calcined at 1123 K for 6 h. Calcined powder was used to make for cylindrical pellets with the using of 2% PVA as a binder on applying 5 tons of pressure using hydraulic pressure for 90 s. Finally, the CCTMO pellets were sintered at 1223 K for 8 h.

Characterization

Thermogravimetric analysis (TGA) of CCTMO powder was used in the air at the heating rate 10 °C/min from room temperature to 1073 K using with the help of thermal analyzer (PerkinElmer, USA). The crystalline phase of CCTMO

ceramic sintered sample was identified by X-ray diffractometer (Rigaku mini flex 600, Japan) applying Cu-kα radiation with wavelength 1.5418 A°. The microstructure and elemental composition were examined by scanning electron microscope (SEM) (ZEISS; model EVO18 research, Germany) attached with energy-dispersive X-ray (EDX) analyzer (Oxford instrument, USA). The average grain size was determined from the respective backscattered SEM images by the averaging size of 50 randomly selected grain on each sample. The particle size was examined by a transmission electron microscope (TEM, Technai G2 20 S-Twin). For TEM characterization, the samples were dispersed in acetone and sonicated 3 h. This suspension was deposited on a carbon-coated copper grid and dried in oven 2 h. The thickness and surface morphology were analyzed using atomic force microscopy (NTEGRA Prima, Germany). The magnetic property of CCTMO was determined by Quantum Design MPMS-3, over a temperature range 5 to 300 K at magnetic field ± 2 T. Temperature difference of zero-field cooled (ZFC) was determined at 100 Oe applied field that was carried out using SQUID VSM dc magnetometer. The dielectric data of silver-coated cylindrical pellets were examined by LCR meter (PSM1735, NumetriQN₄L, and U.K.)

Results and discussion

TGA studies

Thermal decomposition of CCTMO powder carried out by thermogravimetric analysis (TGA) with a heating rate of 10 °C/min from ambient temperature to 1073 K is shown in Fig. 1 from the TGA curve, two stages of weight loss are observed. First, weight loss observes from 503 to 613 K due to incomplete combustion of citric acid and second weight loss occurs in between 873 and 973 K temperatures, maybe due to the formation of an intermediate. The major phase of CCTO along with minor TiO_2 formation observed above 1073 K.

Microstructure studies

Figure 2 shows the X-ray diffraction pattern of CCTMO ceramics sintered at 1223 K for 8 h. The entire diffraction pattern is correctly matched with the JCPDS (card no.21-0140), confirmed the presence of major phase formation of CCTO ceramic having body-centered cubic structure along with the minor secondary phase JCPDS (card no.46-1238) of TiO_2 [22]. The crystalline size (D) of CCTMO was calculated by using the Debye Scherrer formula.

$$D = \frac{K\lambda}{\beta COS\theta} \tag{1}$$

Fig. 1 TGA plot of CaCu$_3$Ti$_3$MnO$_{12}$ as prepared powder
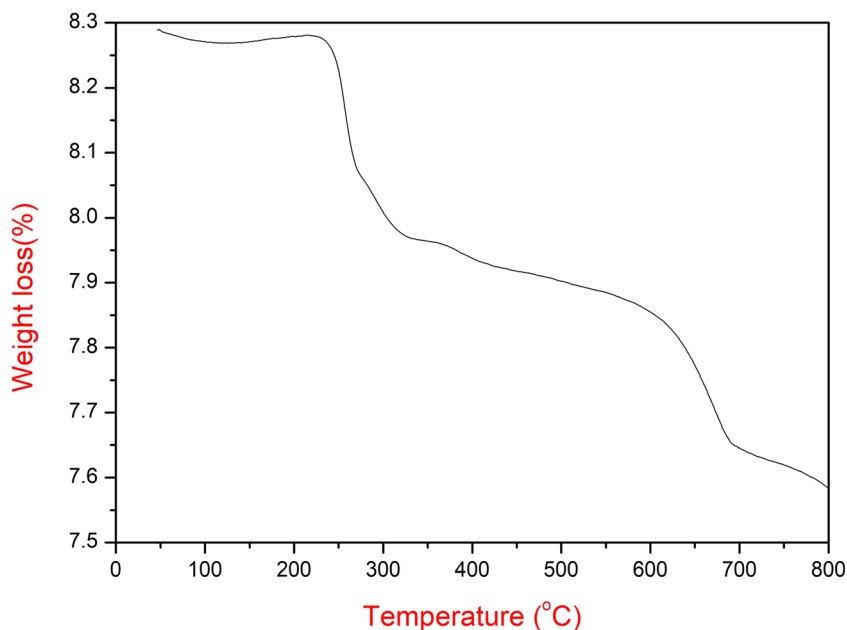
where D is the crystallite size, k is the constant equal to 0.89, λ is the wavelength of X-ray, θ is the Bragg diffraction angle, and β is the full width at half maximum (FWHM) in radians. For the calculation of the correct value of crystallite size, the line broadening due to instrument effect eliminated by using a standard sample for XRD data. The average crystalline size of CCTMO calculated from XRD data is 34.77 ± 10 nm.

Figure 3 shows a bright-field TEM image and selected area diffraction pattern (SEAD) of CCTMO ceramic sintered at 1223 K for 8 h. Figure 3a reveals the nanocrystalline nature of the particles. The observed particle size calculated by TEM measurement is found in the range of 32–75 nm. The particle size observed from TEM is closed to the average crystallite size which is observed by XRD result. The nanocrystalline nature of CCTMO is also confirmed by selected area diffraction (SAED) patterns, shown in Fig. 3b.

The SEM micrograph of a sintered pellet of CCTMO is shown in Fig. 4a, which reveals the clear homogeneous grain formation with the average grain size of 1.46 μm [23]. It is clear from SEM micrograph that smaller grains were observed in nanometer and bigger grain in micrometer range [24]. The elemental composition of CCTMO observed by using electron

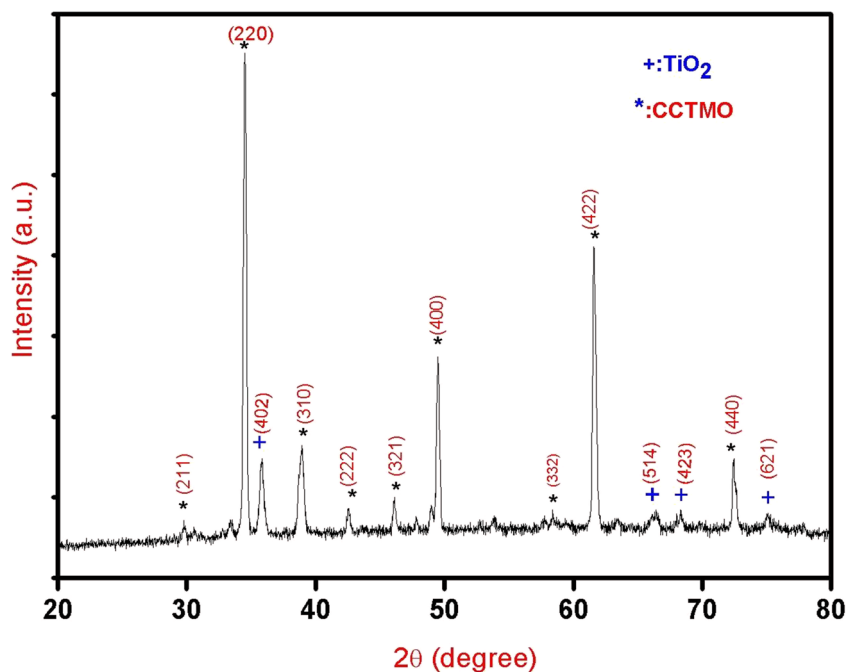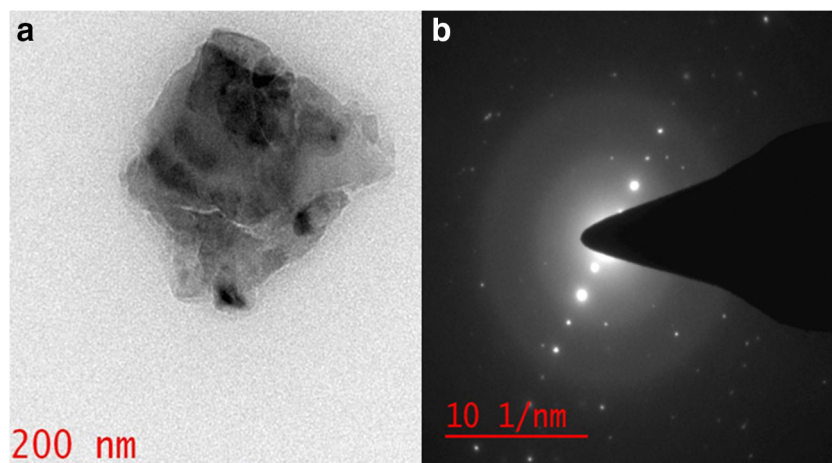**Fig. 2** XRD diffraction pattern of sintered CCTMO at 1223 K for 8 h

Fig. 3 **a** Bright-field TEM images. **b** Selected area diffraction pattern (SEAD) of CCTMO ceramics sintered at 1223 K at 8 h

diffraction X-ray (EDX) spectroscopy is shown in Fig. 4b. The atomic percentage and weight percentage of Ca, Cu, Ti, Mn, and O are found to be 5.62, 14.20, 18.78, 6.67, 54.73 and 6.89, 27.61, 27.52, 11.20, 27.78, respectively. The weight percentage and atomic percentage of CCTMO ceramic confirmed the stoichiometry and the purity of the material.

Figure 5a shows 2D AFM images of CCTMO ceramic sintered at 1223 K for 8 h that explains the cubical structure of grains which is separated by a grain boundary. The average roughness (R_a) and root mean square roughness (R_q) are found to be 0.109 μm and 0.141 μm, respectively, on scanned area 40 μm × 40 μm. Figure 5b exhibits the distribution of particle on the surface that was examined in the 3D structure. The average roughness (R_a) and root mean square roughness (R_q) are found to be 0.163 μm and 0.209 μm, respectively. The maximum peak-valley depth of two-dimensional structure is to be found 0.40 μm. The grain size obtained by the histogram

plots lies in 1–1.6 μm range and average particle size is found to be 0.3 μm out of 513 grains that is shown in Fig. 5c [25].

Dielectric studies

Figure 6a shows the temperature-dependent dielectric constant at a few selected frequencies (1 Hz, 10 kHz, and 100 kHz). It is observed from the figure that the dielectric constant of CCTMO is almost temperature independent from 300 to 500 K at all measured frequency on substitution Mn in CCTO ceramic [26]. The constant value of ε^r with temperature is observed due to the phase transition from ferroelectric to paraelectric. The value of dielectric constant (ε^r) for CCTMO is found to be 50 at 1 kHz. Figure 6b shows the variation of dielectric loss (tan δ) with the temperature at a few selected frequencies. It is clear from the figures that tan δ firstly increases from 300 K and decreases after 390 K. The

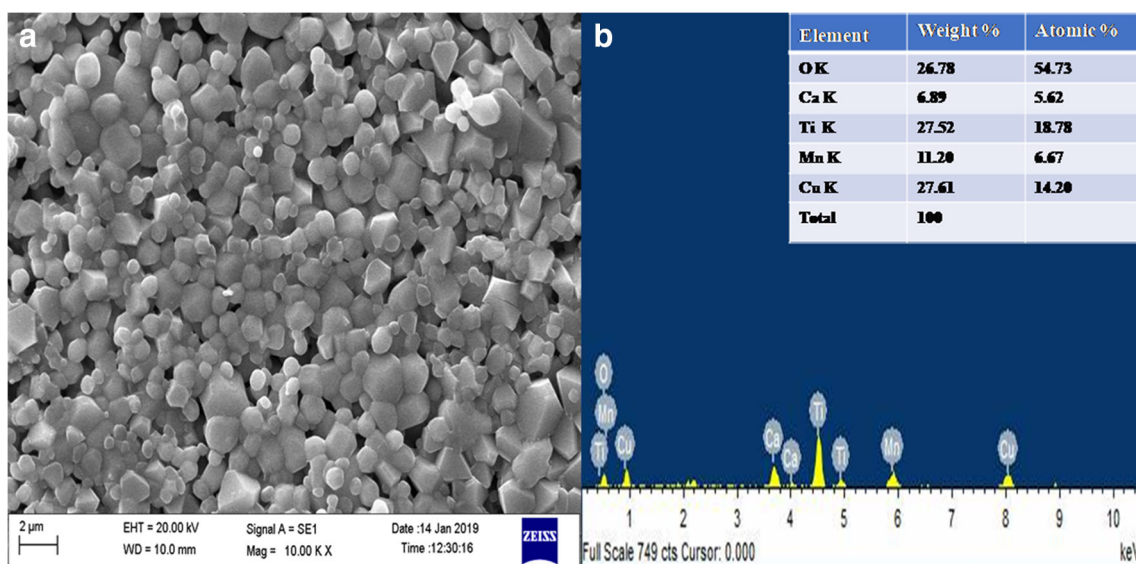| Element	Weight %	Atomic %
O K	26.78	54.73
Ca K	6.89	5.62
Ti K	27.52	18.78
Mn K	11.20	6.67
Cu K	27.61	14.20
Total	100	

Fig. 4 SEM images of CCTMO ceramics sintered at 1223 K for 8 h, **a** SEM images of CCTMO, **b** EDX spectra of CCTMO ceramic
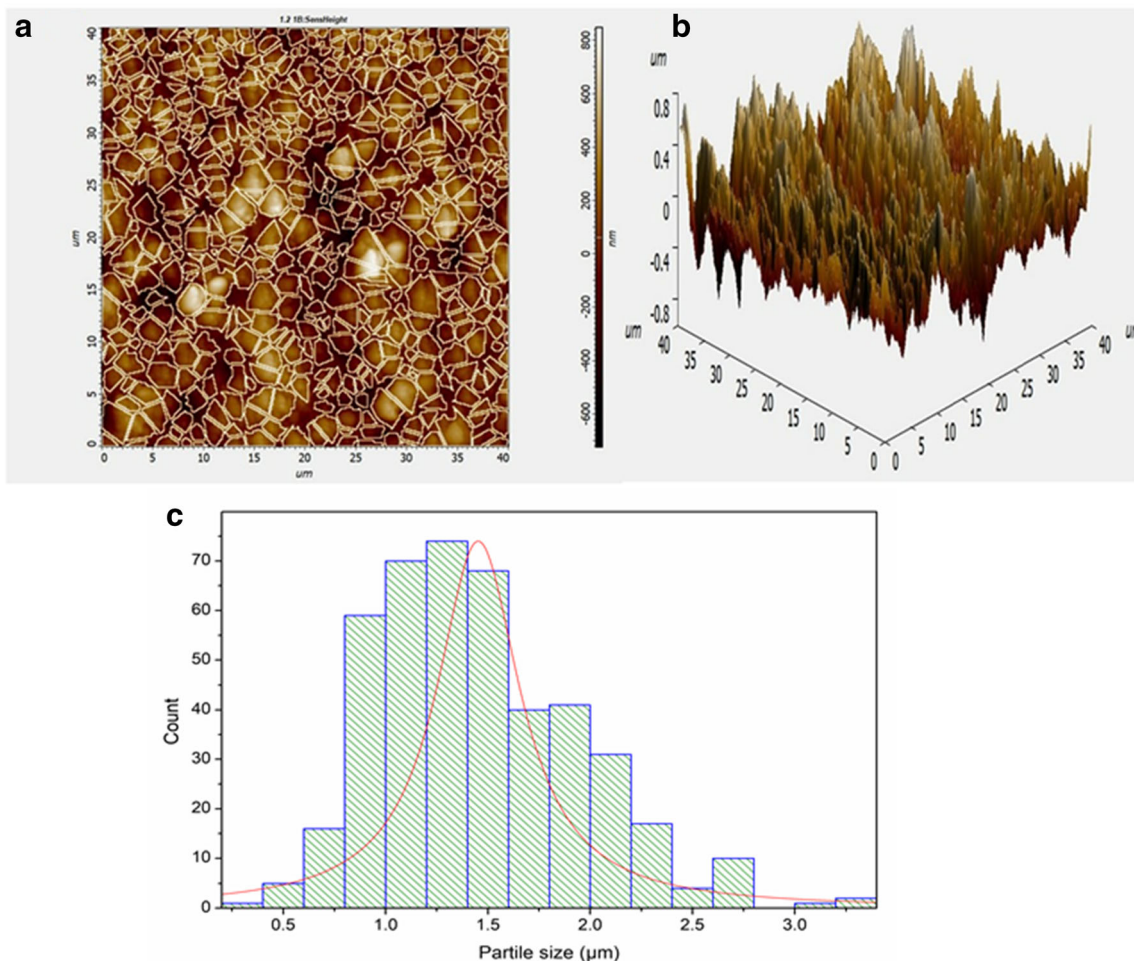
Fig. 5 AFM images of CCTMO ceramics sintered at 1223 K for 8 h, **a** two-dimensional structure, **b** three-dimensional structure, **c** bar diagram of particle size
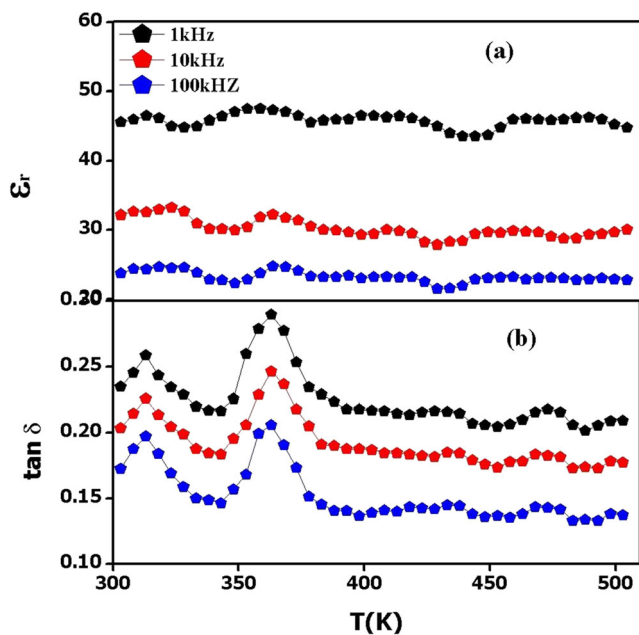

Fig. 6 Temperature-dependent **a** dielectric constant (ε^r) and **b** dielectric loss (tan δ) at a few selected frequencies

value of tan δ of CCTMO is found to be less than 0.233 at all measured frequencies. Figure 7a and b show frequency-dependent permittivity (ε^r) and dielectric loss tangent (tan δ) at few selected temperatures of CCTMO ceramic. Figure 7a shows the permittivity (ε^r) result of CCTMO sample 100 Hz to 1 MHz data that indicate that Mn-doping CCTO shows the low value of permittivity (10^2 at 1 MHz). The decreasing behavior of dielectric constant is explained by Maxwell-Wagner phenomenon [27]. The dielectric constant was found less than 100 at all measured temperature. The low value of the dielectric constant of CCTMO ceramic is due to low conductivity nature of Mn-doped CCTO ceramic. The result indicates that Mn^{4+} partially substituted in place of Ti^{4+} site of CCTO and represented as $CaCu_3Ti_3MnO_{12}$ ceramic shows significant effect in dielectric nature of CCTO [28, 29]. The Mn^{4+} ions enter into both grain and grain boundary; this response is responsible for significant changes in electrical properties of grains and grain boundaries with increasing the Mn^{4+} ion concentration [28, 29]. Figure 7b shows the variation of dielectric loss (tan δ) from 100 Hz to 1 MHz at a few selected temperatures. The value of tan δ of CCTMO was found to be less than 0.1 at all selected temperatures.

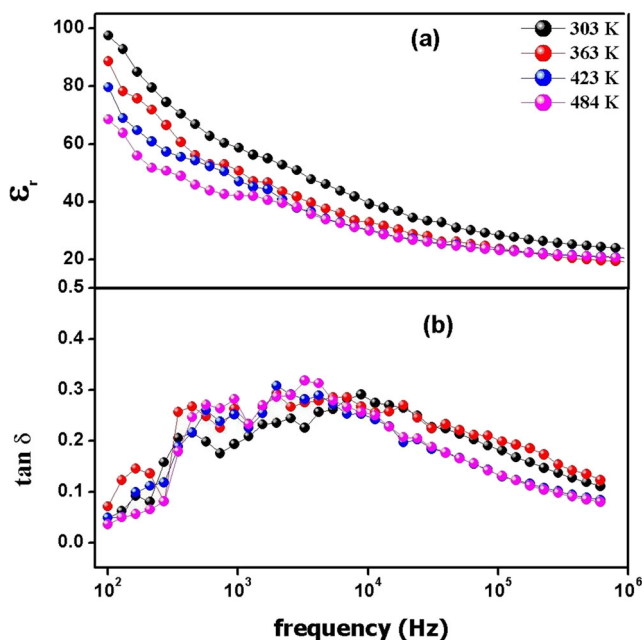**Fig. 7** Frequency-dependent **a** dielectric constant (ε^r) and **b** dielectric loss (tan δ) at few selected temperature

Magnetic studies

Figure 8a depicts the dependence of magnetization of zero-field cooled (ZFC) and field cooled (FC) at the temperature 5 K to 300 K and the applied magnetic field is 100 Oe. The compound shows the transition between ferromagnetic to paramagnetic in natures [30]. The M-T plots (Fig. 8a) show the divergence between ZFC and FC approximately at 30 K. The magnetic behavior increases rapidly in the FC curve which confirms that the presence of ferromagnetic property in Mn-doped CCTO [31]. However, Mn-doped ZFC and FC

curve decreases with increasing temperature. Both ZFC and FC plots show the two different branches which are merged into a tail at the Curie temperature. The Curie temperature for Mn-doped CCTO is found to be 94.37 K. The variation of magnetization (M) with the magnetic field (H) at two different temperatures (5, 300 K) and applied magnetic field ± 2 T for CCTMO is shown in Fig. 8b. M-H hysteresis curves at 5 K temperature explain the ferromagnetic nature, and the linear variation in a magnetic moment with respect to the magnetic field is observed with an increase of temperature (300 K) which confirms the presence of paramagnetic nature of the material. The values of magnetic saturation (M_s), remnant magnetization (M_r), and coercivity (H_c) at a lower temperature (5 K) are calculated and found to be 14.09, 9.93 emu/g, and + 507.088 Oe, respectively [26].

Figure 9 depicts the temperature-dependent reciprocal of magnetic susceptibility for CCTMO ceramic. The Weiss temperature (θ) and Curie constant (C) can be determined by using the fitting of the curve with the help of the Curie–Weiss law, represented by the following equation.

$$\chi = \frac{C}{T-\theta} \tag{2}$$

where χ is the magnetic susceptibility, C is the curie constant, θ is the Curie Weiss temperature, and T is the temperature. The calculated value of Curie constant and Weiss temperature obtained by this plot were found to be 220.6 emu/g^{-1} and 94.37 K, respectively. The positive value of θ indicates the ferromagnetic nature of CCTMO ceramic.

Figure 10 shows the polarization versus electric field (P-E) hysteresis curve of CCTMO ceramic measured at different
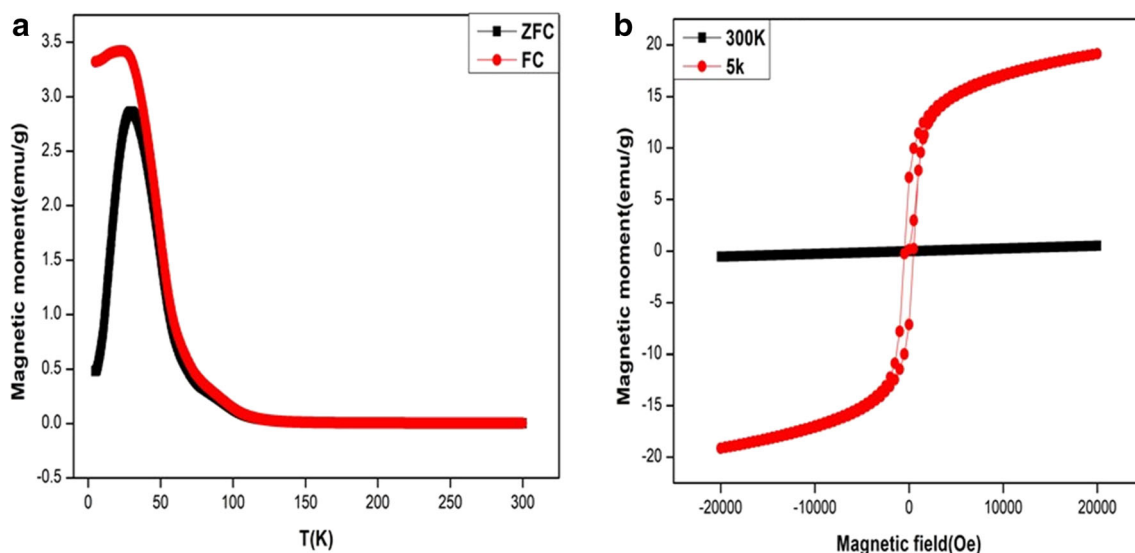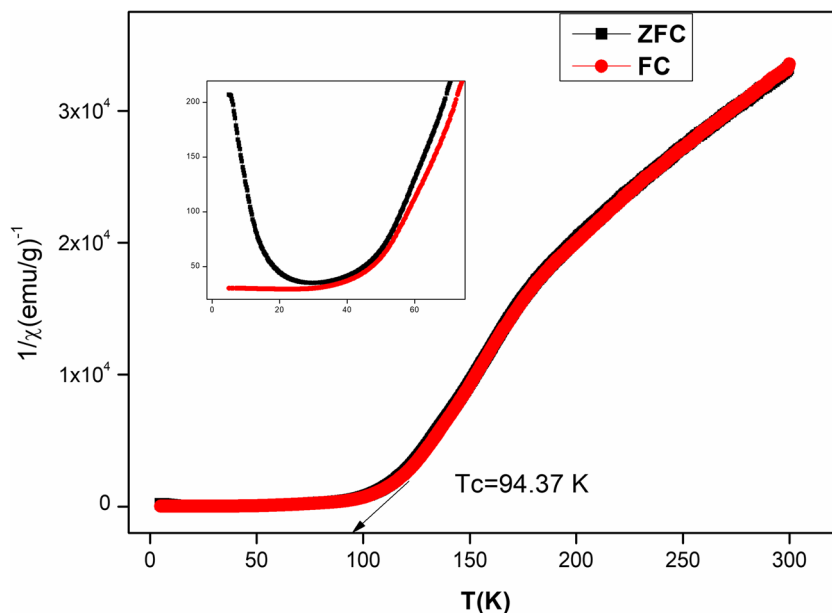

Fig. 8 Temperature-dependent **a** magnetic moment noted at ± 2 T and magnetic field at 100 Oe. **b** M-H hysteresis at 5 and 300 K for CCTMO ceramic

Fig. 9 Magnetic susceptibility as a function of temperature recorded at ± 2 T and applied magnetic field (H) at 100 Oe (inset figure shows zoom view of $1/\chi$ versus T in the range of 0 to 100 K)

temperatures and frequency of 150 Hz. It is observed from the figure that loop shape changes in slimmer with an increase of temperature, which indicates the evolution process to relaxor ferroelectrics. The coercivity value obtained from the P-E hysteresis curve is 2.54, 2.23, 1.641, and 0.806 kV/cm, respectively, at 303 K, 323 K, 343 K, and 364 K, respectively, that explain that the value of Hc decreases with increasing temperature. The measured values of remnant polarizations for CCTMO ceramic are 0.259, 0.275, 0.317, and 0.364 $\mu C/cm^{-2}$, respectively, at the same temperatures. The absence of saturation polarization is described by the combined effect of capacitor and resistor joint in parallel (loosy capacitor) [32].
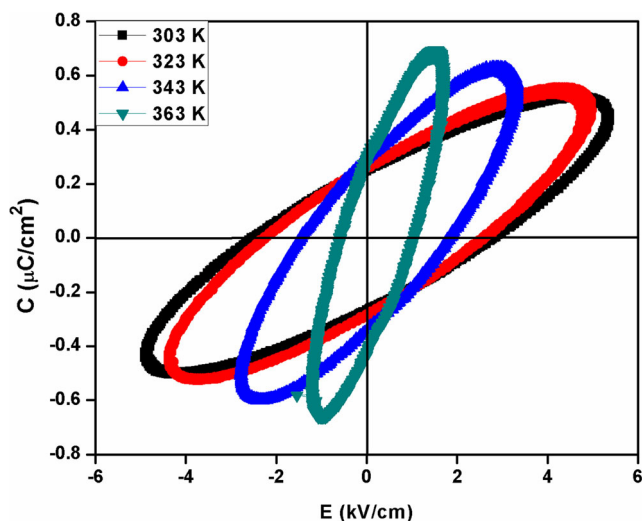
Conclusions

In this summary, manganese doped calcium copper titanium oxide; $CaCu_3Ti_3MnO_{12}$ (CCTMO) was successfully synthesized by using a semi-wet route. Single-phase formation of CCMTO ceramic was confirmed by XRD and average crystallite size obtained from the XRD results was found to be 34.77 ± 10 nm, which is close to the particle size (43.76 ± 10 nm) determined by TEM. The average grain size of sintered materials observed by SEM analysis was 1.46 µm. EDX spectra confirmed the presence of Ca, Cu, Ti, Mn, O element in CCTMO ceramic in stochiometric ratio as the molecular formula. The value of dielectric constant (ε^r) and dielectric loss (tan δ) was found to be 100 and 0.1, respectively, at 303 K and 100 Hz. Magnetic studies emphasized ferromagnetic behavior at lower temperature and attain paramagnetic in nature at a higher temperature.

Fig. 10 P-E hysteresis loop for $CaCu_3TiMnO_{12}$ sintered at 1223 K for 8 h

References

1. Bochu, B., Deschizeaux, M.N., Joubert, J.C., Collomb, A., Chenavas, J., Marezio, M.: Synthèse et caractérisation d'une série de titanates perovskites isotypes de [CaCu3](Mn4) O12. J. Solid State Chem. **29**(2), 291–298 (1979)

2. Windlass, H., Raj, P.M., Balaraman, D., Bhattacharya, S.K., Tummala, R.R.: Colloidal processing of polymer ceramic

nanocomposite integral capacitors. IEEE Trans. Adv. Packag. **26**, 100–105 (2003)

3. Li, J., Subramanian, M.A., Rosenfeld, H.D., Jones, C.Y., Toby, B.H., Sleight, A.W.: Clues to the giant dielectric constant of $CaCu_3Ti_4O_{12}$ in the defect structure of $SrCu_3Ti_4O_{12}$. Chem. Mater. **16**(25), 5223–5225 (2004)

4. Ramirez, A.P., Subramanian, M.A., Gardel, M., Blumberg, G., Li, D., Vogt, T., Shapiro, S.M.: Giant dielectric constant response in a copper-titanate. Solid State Commun. **115**(5), 217–220 (2000)

5. Huang, Y., Shi, D., Li, Y., Li, G., Wang, Q., Liu, L., Fang, L.: Effect of holding time on the dielectric properties and non-ohmic behaviour of $CaCu_3Ti_4O_{12}$ capacitor-varistors. J. Mater. Sci. Mater. Electron. **24**(6), 1994–1999 (2013)

6. Ouyang, X., Habib, M., Cao, P., Wei, S., Huang, Z., Zhang, W., Gao, W.: Enhanced extrinsic dielectric response of TiO2 modified $CaCu_3Ti_4O_{12}$ceramics. Ceram. Int. **41**(10), 13447–13454 (2015)

7. Shay, D.P., Podraza, N.J., Donnelly, N.J., Randall, C.A.: High energy density, high temperature capacitors utilizing Mn-doped $0.8CaTiO_3–0.2CaHfO_3$ ceramics. J. Am. Ceram. Soc. **95**(4), 1348–1355 (2012)

8. West, D.L., Payne, D.A.: Microstructure Development in Reactive-Templated Grain Growth of $Bi_{1/2}Na_{1/2}TiO_3$-Based Ceramics: Template and Formulation Effects. J. Am. Ceram. Soc. **86**(5), 769–774 (2003)

9. Adams, T.B., Sinclair, D.C., West, A.R.: Characterization of grain boundary impedances in fine-and coarse-grained $CaCu_3Ti_4O_{12}$ ceramics. Phys. Rev. B. **73**(9), 094124 (2006)

10. Subramanian, M.A., Li, D., Duan, N., Reisner, B.A., Sleight, A.W.: High dielectric constant in $ACu_3Ti_4O_{12}$ and $ACu_3Ti_3FeO_{12}$ phases. J. Solid State Chem. **151**(2), 323–325 (2000)

11. Singh, L., Sin, B.C., Kim, I.W., Mandal, K.D., Chung, H., Lee, Y.A.: A novel one-step flame synthesis method for tungsten-doped CCTO. J. Am. Ceram. Soc. **99**(1), 27–34 (2016)

12. Li, M., Feteira, A., Sinclair, D.C., West, A.R.: Influence of Mn doping on the semiconducting properties of $CaCu_3Ti_4O_{12}$ ceramics. Appl. Phys. Lett. **88**(23), 232903 (2000)

13. Sinclair, D.C., Adams, T.B., Morrison, F.D., West, A.R.: $CaCu_3Ti_4O_{12}$ one-step internal barrier layer capacitor. Appl. Phys. Lett. **80**(12), 2153–2155 (2000)

14. Li, W., Schwartz, R.W.: ac conductivity relaxation processes in $CaCu_3Ti_4O_{12}$ ceramics: Grain boundary and domain boundary effects. Appl. Phys. Lett. **89**(24), 242906 (2006)

15. Wu, L., Zhu, Y., Par, S., Shapiro, S., Shirane, G., Tafto, J.: Defect structure of the high-dielectric-constant perovskite $CaCu_3Ti_4O_{12}$. Phys. Rev. B. **71**(1), 014118 (2005)

16. Xu, D., He, K., Yu, R., Sun, X., Yang, Y., Xu, H., Yuan, H., Ma, J.: High dielectric permittivity and low dielectric loss in sol-gel derived Zn doped $CaCu_3Ti_4O_{12}$ thin films. Mater. Chem. Phys. **153**, 229–235 (2015)

17. Cho, A., Han, C.S., Kang, M., Choi, W., Lee, J., Jeon, J., Yu, S., Jung, Y.S., Cho, Y.S.: Direct Correlations of Grain-Boundary Potentials to Chemical States and Dielectric Properties of Doped $CaCu_3Ti_4O_{12}$ Thin Films. ACS Appl. Mater. Interfaces. **10**(18), 16203–16209 (2018)

18. Chung, S.Y., Kim, I.D., Kang, S.J.: Strong nonlinear current–voltage behaviour in perovskite-derivative calcium copper titanate. Nat. Mater. **3**(11), 774 (2004)

19. Fang, T.T., Shiau, H.K.: Mechanism for developing the boundary barrier layers of $CaCu_3Ti_4O_{12}$. J. Am. Ceram. Soc. **87**(11), 2072–2079 (2004)

20. Kim, C.H., Jang, Y.H., Seo, S.J., Song, C.H., Son, J.Y., Yang, Y.S., Cho, J.H.: Effect of Mn doping on the temperature-dependent anomalous giant dielectric behaviour of $CaCu_3Ti_4O_{12}$. Phys. Rev. B. **85**(24), 245210 (2012)

21. Thongbai, P., Pinitsoontorn, S., Amornkitbamrung, V., Yamwong, T., Maensiri, S., Chindaprasirt, P.: Reducing loss tangent by controlling microstructure and electrical responses in $CaCu_3Ti_4O_{12}$ ceramics prepared by a simple combustion method. Int. J. Appl. Ceram. Technol. **10**, E77–E87 (2013)

22. Lin, Y.H., Cai, J., Li, M., Nan, C.W., He, J.: High dielectric and nonlinear electrical behaviors in TiO2 -rich Ca $Cu_3Ti_4O_{12}$ ceramics. Appl. Phys. Lett. **88**(17), 172902 (2006)

23. Khare, A., Yadava, S.S., Mandal, K.D., Mukhopadhyay, N.K.: Effect of sintering duration on the dielectric properties of 0.9 $BaTiO_3–0.1$ $CaCu_3Ti_4O_{12}$ nanocomposite synthesized by solid state route. Microelectron. Eng. **164**, 1–6 (2016)

24. Kim, H.E., Choi, S.M., Hong, Y.W.: Improved dielectric properties of the $CaCu_3Ti_4O_{12}$ composites using $BaTiO_3$-coated powder as precursor. J. Alloys Compd. **610**, 594–599 (2014)

25. Gautam, P., Khare, A., Sharma, S., Singh, N.B., Mandal, K.D.: Characterization of $Bi_{2/3}Cu_3Ti_4O_{12}$ ceramics synthesized by semi-wet route. Pro. Nat. Sci-Mater. **26**(6), 567–571 (2016)

26. Wu, X., Huang, K., Yuan, L., Feng, S.: Fabrication of ultralong perovskite structure nanotubes. RSC Adv. **8**(1), 367–373 (2018)

27. George, M., Nair, S.S., Malini, K.A., Joy, P.A., Anantharaman, M.R.: Finite size effects on the electrical properties of sol–gel synthesized $CoFe_2O_4$ powders: deviation from Maxwell–Wagner theory and evidence of surface polarization effects. J. Phys. D. Appl. Phys. **40**(6), 1593 (2007)

28. Jia, R., Zhao, X., Li, J., Tang, X.: Colossal breakdown electric field and dielectric response of Al-doped $CaCu_3Ti_4O_{12}$ ceramics. Mater. Sci. Eng. B. **185**, 79–85 (2014)

29. Sun, D.L., Wu, A.Y., Yin, S.T.: Structure, properties, and impedance spectroscopy of $CaCu_3Ti_4O_{12}$ ceramics prepared by sol–gel process. J. Am. Ceram. Soc. **91**(1), 169–173 (2008)

30. Mo, Z.J., Shen, J., Gao, X.Q., Liu, Y., Wu, J.F., Shen, B.G., Sun, J.R.: Magnetic properties and magnetocaloric effects in HoPd intermetallic. Chinese. Phys B. **24**(3), 037503 (2015)

31. Han, D., Wu, Z., Wang, Z., Yang, S.: Oriented Mn-doped CuO nanowire arrays. Nanotechnology. **27**(13), 135603 (2012)

32. Yadava, S.S., Singh, L., Sharma, S., Mandal, K.D., Singh, N.B.: Effect of temperature on the dielectric and ferroelectric properties of a nanocrystalline hexagonal $Ba_4YMn_3O_{11.5-\delta}$ ceramic synthesized by a chemical route. RSC Adv. **6**(72), 68247–68253 (2016)